

# Force chain splitting in granular materials: A mechanism for large-scale pseudo-elastic behaviour

J.-P. Bouchaud<sup>1,a</sup>, P. Claudin<sup>2,b</sup>, D. Levine<sup>2</sup>, and M. Otto<sup>1</sup>

<sup>1</sup> Service de Physique de l'Etat Condensé, CEA-Saclay, Orme des Merisiers, 91191 Gif-sur-Yvette Cedex, France

<sup>2</sup> Technion - Israel Institute of Technology, Physics Department, Haifa 32000, Israel

Received 13 November 2000 and Received in final form 3 January 2001

**Abstract.** We investigate both numerically and analytically the effect of strong disorder on the large-scale properties of the hyperbolic equations for stresses proposed in J.-P. Bouchaud, M.E. Cates, P. Claudin, *J. Phys. I* **5**, 639 (1995), and J.P. Wittmer, P. Claudin, M.E. Cates, J.-P. Bouchaud, *Nature* **382**, 336 (1996); J.P. Wittmer, P. Claudin, M.E. Cates, *J. Phys. I* **7**, 39 (1997). The physical mechanism that we model is the local splitting of the force chains (the characteristics of the hyperbolic equation) by packing defects. In analogy with the theory of light diffusion in a turbid medium, we propose a Boltzmann-like equation to describe these processes. We show that, for isotropic packings, the resulting large-scale effective equations for the stresses have exactly the same structure as those of an elastic body, despite the fact that no displacement field needs to be introduced at all. Correspondingly, the response function evolves from a two-peak structure at short scales to a broad hump at large scales. We find, however, that the Poisson ratio is anomalously large and incompatible with classical elasticity theory that requires the reference state to be thermodynamically stable.

**PACS.** 05.40.-a Fluctuation phenomena, random processes, noise, and Brownian motion – 45.70.Cc Static sandpiles; granular compaction – 83.70.Fn Granular solids

## 1 Introduction

The mechanics of assemblies of hard, cohesionless grains has been the subject of rather controversial studies in the past few years [1–4]. A well-developed approach, in particular for engineering applications, is based on the assumption that granular materials behave, on large length scales, as elastic (or elastoplastic) bodies. The microscopic justification of this assumption for undeformable cohesionless particles is however far from obvious. The conventional theory of elastic bodies starts from the identification of a reference state from which deformations are defined; the free-energy of the deformed body is then expanded in powers of the strain tensor [5]. The definition of a smooth deformation field and of its energy are both problematic in the context of hard grains [4]. Recent numerical simulations furthermore suggest that a limiting curve relating stresses and deformations for large enough volumes might not even exist [6].

The absence of any obvious deformation field from which the stress tensor may be constructed has motivated an alternative, “stress-only” approach [7, 8, 3, 9]. The basic

tenet of these theories is that in equilibrium, some (history dependent) relations between the components of the stress tensor are established. A well-known relation of this type arises from the assumption that the material is everywhere on the verge of plastic failure, leading to a Mohr-Coulomb relation between the stress components [10]. A simpler relation, based both on symmetry arguments and on the consideration of simple rules for the transfer of stresses between adjacent grains, is a local proportionality between the diagonal components of the stress tensor [7]. For example, in two dimensions, this relation reads  $\sigma_{xx} = c_0^2 \sigma_{zz}$ , where  $c_0$  is a constant. This equation is a local version of the hypothesis made by Janssen in his famous theory for stresses in silos [10, 9, 11]. The consequence of this apparently innocuous assumption is that stresses obey a *hyperbolic* equation, as compared to the elliptic equations encountered in elasticity theory. This means that stresses “propagate” along lines that break rotational symmetry: the characteristics of this hyperbolic equation were argued to be the mathematical transcription of the *force chains* that are well known to exist in granular materials [12]. More elaborate versions of the above closure relation between the components of the stress tensor have been investigated in [8, 9], and have been shown to reproduce both the pressure “dip” underneath the apex of a sandpile [13, 14], or the pressure profile inside silos [11].

<sup>a</sup> e-mail: bouchau@spec.saclay.cea.fr

<sup>b</sup> *Present address:* Laboratoire des Milieux Désordonnés et Hétérogènes, 4 place Jussieu, case 86, 75252 Paris Cedex 05, France.

A rather clear-cut difference between hyperbolic and elliptic equations lies in the structure of the propagator, *i.e.* the response of the stress to a localized force applied at the top of a layer of granular matter of height  $h$ . For a hyperbolic equation, the pressure profile at the bottom of the layer is localized around two peaks (in two dimensions) or a circular annulus (in three dimensions), centred underneath the point where the force is applied [7]. For an elliptic equation, by contrast, the response function is a bell-shaped curve of width  $\propto h$  that reaches its maximum precisely underneath the point where the force is applied. A similar single-peak structure, but of width  $\propto \sqrt{h}$ , is also predicted by scalar models [15], where the stress obeys a (parabolic) diffusion equation.

This response function has only very recently been carefully measured experimentally. For well-ordered packings, or for frictionless beads, the two-peak structure is rather convincingly observed both in two and three dimensions [16,17], and has been further justified theoretically in [18]. However, as soon as the packing is disordered (for example, by considering mixtures of grains of different sizes), the two-peak structure disappears on large length scales and is replaced by a one-peak, elastic-like, response function [19,16,20], with a width scaling as  $h$ . This single hump response function has also been observed in numerical simulations of disordered packing in [21]. Finally, a purely diffusive response function (scaling as  $\sqrt{h}$ ) was reported in [22], but on a very special “brick” packing.

The aim of this paper is to investigate both numerically and theoretically the consequences of strong disorder on the large-scale properties of the locally hyperbolic equations proposed in [7,8]. We propose and simulate numerically a simple model where force chains only locally propagate in straight lines as in Edwards’ picture [23] or in hyperbolic models [7,8], and are occasionally scattered by defects. This model can be seen as an assembly of “grains” (in a metallurgic sense) with randomly oriented local propagation directions. At each “grain boundary”, incoming force chains scatter into the new propagation directions. The response function is seen to evolve, as a function of the height  $h$  of the layer, from a two-peak (anisotropic) structure at small scales to a one-peak (isotropic) elastic-like response at large scales.

We then propose a Boltzmann-like formalism to describe the statistics of this force chain scattering process. We show that the large-scale effective equations for the stresses become elliptic, and, rather surprisingly, have *exactly the same structure as the equations governing the stresses in an elastic body*. This is quite striking because no displacement field needs to be introduced at all. (This is actually also true of our numerical model where only forces are considered.) Interestingly, it is the very existence of force chains that allows one to define a local vectorial “order parameter” (that we call  $\mathbf{J}$  below) which formally plays the role of the displacement in elasticity theory. The importance of force chains for the mechanics of granular materials was emphasized in [23,12]; the present work suggests that their presence might be (somewhat

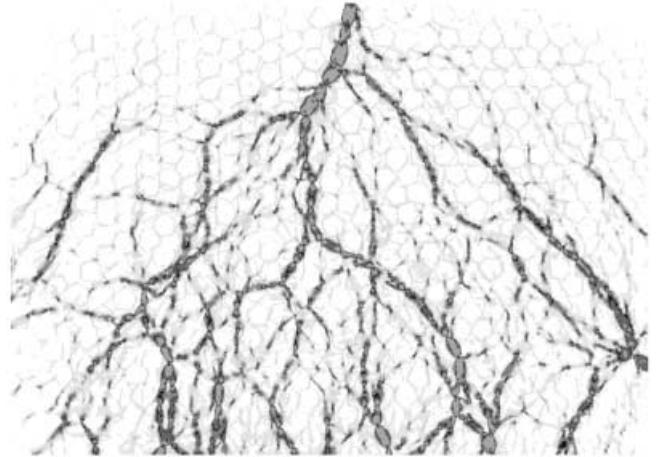


**Fig. 1.** Picture of the force chains in a two-dimensional system of grains subject to a vertical force imposed at the middle of the top surface [20]. Such a picture has been obtained with birefringent grains between inverse circular polarizers.

paradoxically) crucial to allow for a large-scale elastic-like behaviour.

The Poisson ratio  $\nu$  that appears in our elastic-like equations depends solely on the statistical properties of the force chain splitting process. Interestingly, this Poisson ratio violates the bound  $\nu \leq 1/2$  (in three dimensions) that comes from the fact that the elastic energy of deformations is a positive quadratic form of the strain tensor. This clearly shows that although the final equations have the same formal structure as those of elasticity theory, granular materials do not behave as standard elastic bodies, even for statistically isotropic packings. Note that boundary conditions are also different.

## 2 The force-splitting model: definition and numerical simulations

Pictures of photoelastic grains under compression clearly reveal the existence of linear force chains which tend to split upon meeting vacancies or packing defects: see Figure 1 [24,25]. This motivates the following model to compute the response function  $G(x, h)$  to a force imposed at the top of the layer ( $x = 0, z = 0$ ), and measured at  $x$  and  $z = h$ . For a perfectly ordered packing, we want this response to be made of two sharp peaks centered at  $x = \pm c_0 h$ , where  $c_0 = \tan \theta_0$  is the tangent of the angle of the direction along which forces are transmitted in regular arrangement of grains. For a compact triangular packing, this angle is  $\theta_0 = 30^\circ$ , which is the value that we choose in the following simulations. Therefore we start with two force chains at angle  $\pm \theta_0$  to the vertical. For disordered packing, we randomly distribute non-overlapping defects of radius  $a = 1$  (this fixes the unit length) with a density  $\rho_d$ . If one of the force chains meets a defect, we split it into two new ones at random angle, corresponding to a new local orientation of the underlying hyperbolic model.

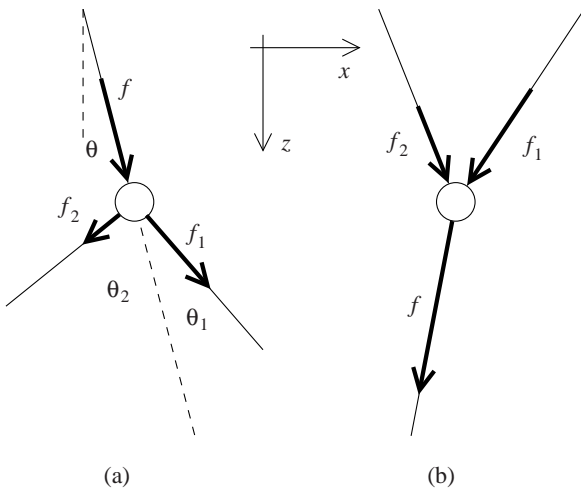


**Fig. 2.** The disorder of the packing is modelled by the presence of “defects” where force chains can split at random angles (a) (“ $\lambda$  processes”) —or merge (b) (“ $Y$  processes”). The force chains have no width, but the defects have a finite radius  $a = 1$ . At each defect, forces are balanced:  $f\mathbf{n} = f_1\mathbf{n}_1 + f_2\mathbf{n}_2$ .

These two chains then propagate until another defect (or the boundary) is reached, and so on.

More precisely, a chain carrying a force  $f$  in the direction  $\mathbf{n}$  splits, when meeting a defect, into two forces  $f_1, f_2$  in the directions  $\mathbf{n}_1, \mathbf{n}_2$ . The two angles  $\theta_1$  and  $\theta_2$  (between  $\mathbf{n}$  and  $\mathbf{n}_1$  and  $\mathbf{n}_2$ , respectively) are uniformly chosen between 0 and some maximum splitting angle  $\theta_M$ . The local mechanical equilibrium imposes that the intensities  $f_1$  and  $f_2$  are such that  $f\mathbf{n} = f_1\mathbf{n}_1 + f_2\mathbf{n}_2$  —see Figure 2(a). Sometimes, two (or more) force chains meet at the same defect. In this case, we make them all merge together —see Figure 2(b). It is important to note that the positions of the defects are fixed before starting the computation of the forces. This idea of a frozen disorder is consistent with the experimental observation that when the local overload is added on the top of the system, the forces are transmitted along the chains originally created during the building of the packing. In other words, as long as the applied force is not too large and compatible with the pre-existing network of force chains, the geometry of the packing, and in particular the contacts between grains, remains the same.

The network of forces is built in a hierarchical manner: each defect involved in this network has one or more “parents” and one or more “children”. The most common situation is when a defect has one parent and two children. We define such defects to be of “ $\lambda$  type”. Defects of “type  $Y$ ” have two (or, very rarely, three or more) parents but one child only. Finally, some defects are not involved in the network of forces. The type of defects is not fixed *a priori*. At the beginning of the calculation, all defects are “free” and become progressively of  $\lambda$  type when reached by a force chain. When a force chain reaches a defect which is already of  $\lambda$  type (or, less likely, of  $Y$  type), all force chains originally descending from this defect are removed, and it

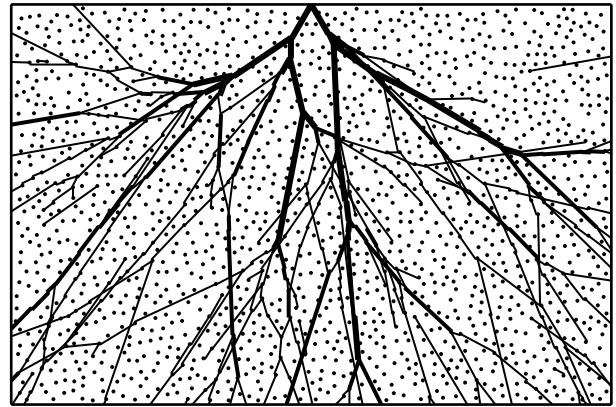


**Fig. 3.** Snapshot of the network of force chains obtained within the  $\lambda Y$  model. The dots represent the defects of the granular packing. The lines are bolder when the forces are larger —very small forces (less than 0.01) have not been plotted. In this picture we set the height to  $h = 200$ , the width to  $2w = 300$ , the density of defects to  $\rho_d = 0.028$  and the maximum splitting angle to  $\theta_M = 30^\circ$ .

becomes of  $Y$  type. Note that this procedure does not allow cycles, *i.e.* defects cannot be their own ancestors —or descendants<sup>1</sup>. We checked that the final network of force chains is independent of the order in which defects are chosen at each step. Eventually, all the force chains reach a boundary of the system, and the calculation stops. All four walls are perfect absorbing boundaries.

A further technical difficulty is the presence of very small forces. The deeper the layer, the larger the number of force chains that carry extremely weak forces. In order to keep the computation time to reasonable values, the total number of force chains cannot grow indefinitely. We therefore introduced a lower cut-off, below which force chains are no longer taken into account. We checked that for small enough cut-off our results are independent of this cut-off.

With these rules, realistic force networks can be created —see Figure 3. After averaging over many statistically identical samples, one can obtain stress profiles for different heights  $h$ . Figure 4 shows that, as  $h$  increases, the vertical pressure response profile evolves continuously from two well-defined peaks to a single broad one. It means that the hyperbolic behaviour is progressively erased by multiple scattering. Besides, the width of the single peak scales like  $h$  —see Figure 5. This scaling is in very good agreement with experiments [16, 19, 20] and rules out an analysis both in terms of the so-called telegrapher’s equation, which was proposed in [26] to interpolate between a locally hyperbolic behaviour, and a large-scale diffusive behaviour implied by scalar descriptions [15, 22].

More precisely, we show that the shape of this peak is not Gaussian: see the inset of Figure 5. Rather, it is surprisingly close to the pure elastic response of a semi-

<sup>1</sup> Even if cycles were to be allowed, the problem would converge very quickly —there is no sense in which allowing cycles would modify, except infinitesimally, the results obtained.

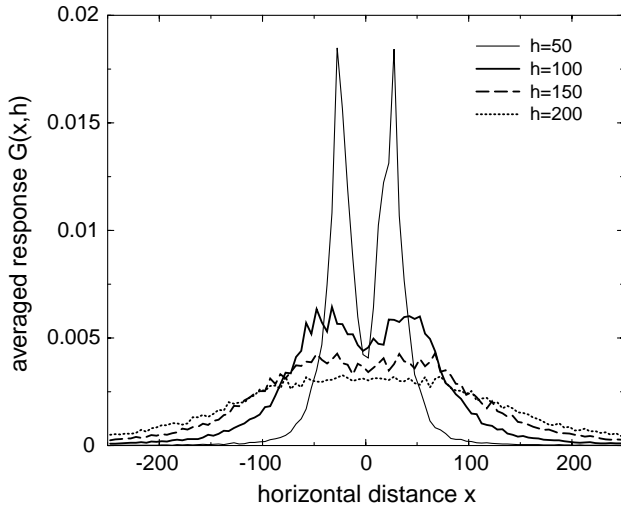


**Fig. 4.** Averaged vertical stress response function for different values of  $h$ . At small scale, the response function has a double-peak shape which is characteristic of a locally hyperbolic behaviour. For larger heights, these two peaks merge into a single broad peak, comparable to an elastic-like response. These curves have been obtained with  $2w = 500$ ,  $\rho_d = 0.028$ ,  $\theta_M = 30^\circ$ , and averaged over 1000 samples.

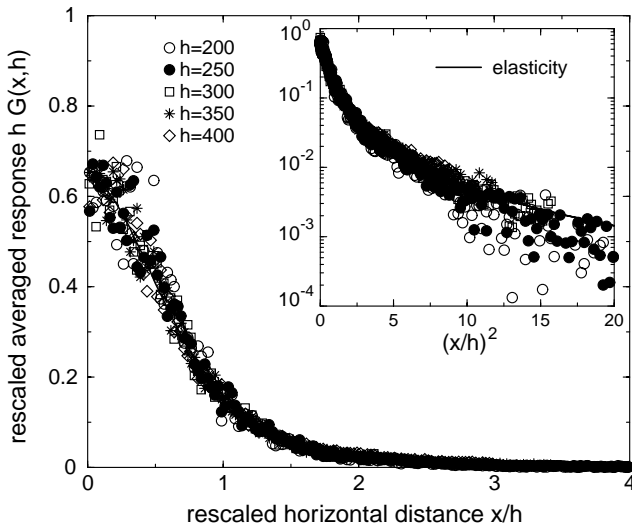


**Fig. 5.** For large heights, the width of the response function grows like  $h$ . The inset shows that its shape is not Gaussian and actually rather close to a purely elastic response, shown as the plain line. These curves have been obtained with  $2w = 2400$ ,  $\rho_d = 0.028$ ,  $\theta_M = 30^\circ$ , averaged over 100 samples, and their integrals normalized to unity.

infinite medium, which reads [5]:

$$G_e(x, h) = \frac{2}{\pi h} \frac{1}{[1 + (x/h)^2]^2}, \quad (1)$$

independently of both the Young modulus and the Poisson ratio. Note that, because some force chains are deflected upwards and reach the top of the system, the integral of

the vertical pressure over the bottom wall  $z = h$  gives a result slightly larger than 1 (typically 1.07 for  $h = 400$  and  $\theta_M = 30^\circ$ ). For a proper comparison with the elastic response, we have renormalized the data so that its integral is unity. However, one should emphasize that the “backward” propagation of forces is a realistic effect. The top layer only remains stable as long as these forces do not exceed the weight of a single grain. For larger applied forces, one expects the top layer to become unstable. Let us now turn to an analytical derivation of the numerical results obtained above.

### 3 A Boltzmann equation for force chain splitting

The role of disorder on hyperbolic equations was previously investigated in [27], where the constant  $c_0$  in the equation relating  $\sigma_{zz}$  and  $\sigma_{xx}$  was allowed to be randomly fluctuating in space. The study was restricted to small fluctuations (*i.e.*  $c_0(\mathbf{r}) = \bar{c}_0 + \delta c(\mathbf{r})$ , with  $\delta c \ll \bar{c}_0$ ), where perturbation theory is valid. In this case, the two-peak structure of the response function is preserved on large length scales, although the peaks are broadened. An uncontrolled extrapolation to strong disorder, however, suggested that the large-scale equations might become elliptic in this regime.

The chain-splitting model proposed above allows us to investigate the strongly disordered situation. Our strategy is to write a Boltzmann equation for the probability density  $P(f, \mathbf{n}, \mathbf{r})$  of finding an oriented force chain of intensity  $f$  in the direction  $\mathbf{n}$  around the point  $\mathbf{r}$ . This probability is defined, as for the numerical results presented above, as an average over different samples with the same boundary conditions. However, one expects that on large length scales, the resulting hydrodynamical equations are self-averaging, *i.e.*, independent of the specific sample. A very important point here is that force chains can be oriented with reference to the boundary conditions. It is indeed a specific property of hyperbolic equations to require boundary conditions either in the “past” or in the “future”, but not in both (see the discussion in [4, 18]). The possibility to orient the chains has been implicitly used in the above numerical scheme.

For simplicity, we shall in the following neglect the chain “merging”  $\Upsilon$  process, and furthermore that the splitting is symmetric, *i.e.* that  $\mathbf{n} \cdot \mathbf{n}_1 = \mathbf{n} \cdot \mathbf{n}_2 \equiv \cos \theta$ , so that  $f_1 = f_2 = f/2 \cos \theta$ . As will be clear from the treatment below, more complicated cases, with more than two offsprings or asymmetric scattering do not change the structure of the large-scale equations, provided the scattering is isotropic on average. (Anisotropic scattering can arise in granular materials with a non-trivial contact texture, and leads to very interesting generalisations that will be mentioned in the conclusion.)

Assuming a uniform density of defects, the probability distribution  $P(f, \mathbf{n}, \mathbf{r})$  obeys the following general

equation:

$$P(f, \mathbf{n}, \mathbf{r} + \mathbf{n}dr) = \left(1 - \frac{dr}{\lambda}\right) P(f, \mathbf{n}, \mathbf{r}) + 2\frac{dr}{\lambda} \int d\mathbf{n}' \int df' P(f', \mathbf{n}', \mathbf{r}) \Psi(\mathbf{n}', \mathbf{n}) \delta\left(f - \frac{f'}{2\cos\theta}\right), \quad (2)$$

where  $\lambda$  is equal to the “mean free path” of force chains, and is of order  $1/(\rho_d a^{D-1})$  in dimension  $D$ . The above equation means the following: since a chain of grains can only transport a force parallel to itself [12], the direction of the force  $\mathbf{n}$  also gives the local direction of the chain. Between  $\mathbf{r}$  and  $\mathbf{r} + \mathbf{n}dr$ , the chain can either carry on undisturbed, or be scattered. The second term on the right-hand side therefore gives the probability that a force chain initially in direction  $\mathbf{n}'$  is scattered in direction  $\mathbf{n}$ . This occurs with a probability  $\frac{dr}{\lambda} \Psi(\mathbf{n}', \mathbf{n})$ , where  $\Psi$  is the scattering cross-section, which we will assume to depend only on the scattering angle  $\theta$ , for example a uniform distribution between  $-\theta_M$  and  $+\theta_M$ . The  $\delta$ -function ensures force conservation and the factor two comes from the counting of the two possible outgoing force chains.

Let us now multiply equation (2) by  $f$  and integrate over  $f$ . This leads to an equation for the local average force per unit volume in the direction  $\mathbf{n}$ , that we will denote  $F(\mathbf{n}, \mathbf{r})$ . This equation reads:

$$\lambda \mathbf{n} \cdot \nabla_r F(\mathbf{n}, \mathbf{r}) = -F(\mathbf{n}, \mathbf{r}) + \int d\mathbf{n}' \frac{F(\mathbf{n}', \mathbf{r})}{\mathbf{n} \cdot \mathbf{n}'} \Psi(\mathbf{n}', \mathbf{n}) + \frac{\lambda}{a} \mathbf{n} \cdot \mathbf{F}_0(\mathbf{r}), \quad (3)$$

where we have added the contribution of an external body force density  $\mathbf{F}_0(\mathbf{r})$ , and  $a$  is the size of a defect or of a grain. This equation is the so-called Schwarzschild-Milne equation for radiative transfer, describing the evolution of light intensity in a turbid medium [28]. We now introduce some angular averages of  $F(\mathbf{n}, \mathbf{r})$  that have an immediate physical interpretation:

$$p(\mathbf{r}) = a \int d\Omega F(\mathbf{n}, \mathbf{r}), \quad (4)$$

$$J_\alpha(\mathbf{r}) = a \int d\Omega n_\alpha F(\mathbf{n}, \mathbf{r}), \quad (5)$$

$$\sigma_{\alpha\beta}(\mathbf{r}) = aD \int d\Omega n_\alpha n_\beta F(\mathbf{n}, \mathbf{r}), \quad (6)$$

where  $\int d\Omega$  is the normalized integral over the unit sphere, that is introduced for a correct interpretation of  $\sigma$  (see Eq. (11) below). As will be clear from the following,  $\mathbf{J}$  is the local average force chain intensity per unit surface,  $\sigma$  is the stress tensor. Since  $\mathbf{n}^2 = 1$ , one finds that  $\text{Tr} \sigma = Dp$ , and therefore  $p$  is the isostatic pressure. Note that  $\mathbf{J}$  is not the average local force, which is always zero in equilibrium. The fact that  $\mathbf{J} \neq \mathbf{0}$  comes from the possibility of orienting the force chains.

#### 4 The hydrodynamic limit: back to “elasticity”

Let us indeed integrate over the unit sphere equation (3) after multiplying it by different powers of  $n_\alpha$ . Using the

fact that  $\Psi(\mathbf{n}', \mathbf{n})$  only depends on  $\mathbf{n} \cdot \mathbf{n}'$ , a direct integration leads to

$$\lambda \nabla \cdot \mathbf{J} = (a_0 - 1)p, \quad (7)$$

where  $a_0$  is called the “albedo” in the context of light scattering [28], and reads:

$$a_0 \equiv \int d\mathbf{n} \frac{\Psi(\mathbf{n}', \mathbf{n})}{\mathbf{n} \cdot \mathbf{n}'} \geq 1. \quad (8)$$

A second set of equations can be obtained by multiplying by  $n_\alpha$  and integrating. Using the fact that

$$a_1 = \int d\mathbf{n} \Psi(\mathbf{n}', \mathbf{n}) = 1, \quad (9)$$

it is easy to show that

$$\int d\mathbf{n} \mathbf{n} \frac{\Psi(\mathbf{n}', \mathbf{n})}{\mathbf{n} \cdot \mathbf{n}'} = \mathbf{n}'. \quad (10)$$

Therefore, the resulting equation is nothing but the usual mechanical equilibrium relation:

$$\nabla_\beta \sigma_{\alpha\beta} = F_{0\alpha}. \quad (11)$$

This relation reflects the local balance of forces chains. Now we multiply equation (3) by  $n_\alpha n_\beta$  and again integrate. *A priori*, this introduces a new three-index tensor. In order to close the equation, we now make the assumption that is usually made in the context of light diffusion, that on large scales the force intensity becomes nearly isotropic [28]. In this case, it is justified to expand  $F(\mathbf{n}, \mathbf{r})$  in angular harmonics and to keep only the first terms<sup>2</sup>:

$$a F(\mathbf{n}, \mathbf{r}) = p(\mathbf{r}) + D\mathbf{n} \cdot \mathbf{J}(\mathbf{r}) + \frac{D+2}{2} \mathbf{n} \cdot \hat{\sigma} \cdot \mathbf{n} + \dots, \quad (12)$$

where  $\hat{\sigma}$  is the deviatoric stress tensor. Equation (12) is similar to the Chapman-Enskog expansion in the context of the Boltzmann equation. The calculation requires the following identity:

$$\Gamma_{\alpha\beta\gamma\delta} \equiv \int d\Omega n_\alpha n_\beta n_\gamma n_\delta = K_1 [\delta_{\alpha\beta} \delta_{\gamma\delta} + \delta_{\alpha\gamma} \delta_{\beta\delta} + \delta_{\alpha\delta} \delta_{\beta\gamma}], \quad (13)$$

where  $K_1 = 1/D(2+D)$ . The resulting equation finally leads to

$$\lambda D \Gamma_{\alpha\beta\gamma\delta} \nabla_\gamma J_\delta = \frac{a_0 - a_2}{D-1} p \delta_{\alpha\beta} + \left( \frac{D a_2 - a_0}{D-1} - 1 \right) \frac{\sigma_{\alpha\beta}}{D}, \quad (14)$$

where

$$a_2 = \langle \cos^2 \theta \rangle \equiv \int d\mathbf{n} \Psi(\mathbf{n}', \mathbf{n}) \mathbf{n} \cdot \mathbf{n}'. \quad (15)$$

<sup>2</sup> Actually, the term in  $\hat{\sigma}$  does not contribute to the following closure equation. Only the third-order term (in  $nnn$ ) would change the following results.

Taking the trace of equation (14), we find, using the fact that the trace of  $\sigma$  is equal to  $Dp$ ,

$$\lambda \nabla \cdot \mathbf{J} = \left( \frac{a_0 - a_2}{D-1} D + \frac{Da_2 - a_0}{D-1} - 1 \right) p, \quad (16)$$

which, using the values of  $K_1$  and  $K_2$ , can be seen to be identical to the first equation, equation (7). The final equation appears therefore as a “constitutive” relation between  $\sigma_{\alpha\beta}$  and the vector  $\mathbf{J}$ . We find

$$\sigma_{\alpha\beta}|_{\alpha \neq \beta} = \frac{\lambda D^2 K_1}{\left( \frac{Da_2 - a_0}{D-1} - 1 \right)} (\nabla_\alpha J_\beta + \nabla_\beta J_\alpha), \quad (17)$$

and

$$\sigma_{\alpha\alpha} = \frac{\lambda D}{\left( \frac{Da_2 - a_0}{D-1} - 1 \right)} \left[ 2DK_1 \nabla_\alpha J_\alpha + \left( DK_1 - \frac{a_0 - a_2}{(D-1)(a_0 - 1)} \right) \nabla \cdot \mathbf{J} \right] \quad (18)$$

(here  $\alpha$  is not summed over.) These equations have exactly the canonical form of elasticity theory, provided one identifies the vector  $\mathbf{J}$  with the local displacement, up to an arbitrary multiplicative factor (note that  $\mathbf{J}$  does *not* have the dimensions of a displacement). Since the quantities  $a_0$  and  $a_2$  are integrated over  $\mathbf{n}$ , different choices for the scattering probability  $\Psi$  would lead to different numerical coefficients, but would not change the elliptic nature of the equations. The effective Young modulus is proportional to  $\lambda / \left( \frac{Da_2 - a_0}{D-1} - 1 \right)$ , up to the arbitrary multiplicative factor mentioned above. However, the Poisson ratio  $\nu$  is independent of this multiplicative factor, and reads:

$$\nu = \frac{1}{D-1} \frac{D-1 + 3a_0 - (D+2)a_2}{D+1 + a_0 - (D+2)a_2}. \quad (19)$$

Note that this quantity is purely geometric, and does not involve the scattering mean free path  $\lambda$ . Since  $a_0 \geq 1$  and  $a_2 \leq 1$ , it is easy to show that  $\nu \geq 1/(D-1)$  in all dimensions, therefore violating the thermodynamical bound  $\nu \leq 1/(D-1)$  that holds for conventional elastic bodies. This means that the stress equations cannot be derived from the minimisation of a free energy functional. Therefore, granular materials (if describable by the present theory) should have an anomalously high Poisson ratio. The Poisson ratio for a uniform distribution of scattering angles is plotted as a function of the maximum angle  $\theta_M$  in Figure 6, both for  $D = 2$  and  $D = 3$ . In the weak scattering limit ( $\theta_M \rightarrow 0$ ), one finds  $\nu = (D+5)/[(D+3)(D-1)]$  independently of the precise shape of  $\Psi$ . In the strong scattering limit where  $\theta_M \rightarrow \pi/2$ , outgoing force chains can carry arbitrarily large forces and therefore  $a_0 \rightarrow \infty$ . In this case,  $\nu \rightarrow 3/(D-1)$ . Such anomalous values of the Poisson ratio in granular materials were discussed in recent papers [29], although the underlying mechanisms are different from the one proposed here.

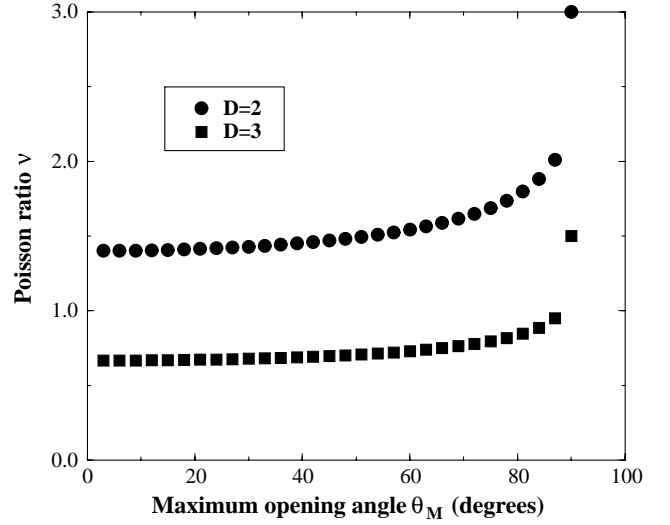


**Fig. 6.** Poisson ratio  $\nu$  for a uniform distribution of scattering angles, as a function of the maximum angle  $\theta_M$ , both for  $D = 2$  (circles) and  $D = 3$  (squares).

Since the above equations are formally identical to those of classical elasticity, one can show that  $\nabla^2 p = 0$ , and  $\nabla^4 \mathbf{J} = 0$  [5]. The corresponding boundary conditions can be derived from the knowledge of the direction of force chains at the boundaries, which determines  $P(f, \mathbf{n}, \mathbf{r})$ . One can therefore compute the response function  $G(\mathbf{r})$  to a localized force at  $\mathbf{r} = 0$  in the  $z$  direction, which is given in  $D = 2$  by equation (1), and is, as Figure 5 shows, in extremely good agreement with the numerical simulation of our force chain splitting model. This response function is also very close to the one measured experimentally [20, 19, 16] or numerically in disordered packings [21].

## 5 Conclusion and extensions

In this paper, we have shown that in the presence of strong disorder that “scatters” the force chains in an assembly of undeformable, cohesionless grains, the locally hyperbolic (and therefore anisotropic) character of the stress equations is unstable on large length scales, where isotropy is restored and the resulting equations become formally identical to those of a conventional elastic body. This is at variance with the weak disorder calculations presented in [27], and shows that the unintuitive two-peak nature of the response function is perhaps restricted to very ordered packings, or frictionless particles, for which  $\lambda \rightarrow \infty$ .

Let us stress once more that our result is not trivial because no displacement field is introduced in the above derivation (nor in our numerical model). The basic assumption of our model is the existence of local force chains, which have a well-defined identity over several grain sizes  $a$ , such that  $a \ll \lambda$ : this is the condition under which the above Boltzmann description of the force chain scattering is justified. Interestingly, chains that propagate the forces parallel to themselves are the signature of a

locally hyperbolic equation, and are associated with its characteristics [12, 9].

This work can be extended in several directions. First, and most importantly, the extension to non-isotropic scattering should be worked out. This means that the scattering function  $\Psi(\mathbf{n}, \mathbf{n}')$  could depend not only on  $\mathbf{n} \cdot \mathbf{n}'$  but also on  $\mathbf{N} \cdot \mathbf{n}'$ , where  $\mathbf{N}$  is a (space dependent) director that describes the local texture, *i.e.* the non-isotropic distribution of contacts between grains. In this case, we find equations similar to those appearing in anisotropic elasticity theory [30]. The director  $\mathbf{N}$  is expected to encode the construction history of the material, and should be non-trivial, for example, in a sandpile constructed from a point source. The modification of the above theory to account for texture effects is needed to understand the existence of the pressure dip underneath the apex of the pile [13, 14], which cannot be reproduced by an isotropic elastic theory (see the discussion in [2, 31]). In the presence of a long-ranged texture field  $\mathbf{N}$ , the response function will depart from that of elasticity theory. Second, the fluctuations of stresses in granular materials are very important and have been discussed theoretically and experimentally [15]. The above theoretical framework should allow to make some progress, by studying higher moments of the local force distribution  $P(f, \mathbf{n}, \mathbf{r})$ , beyond the average force  $F(\mathbf{n}, \mathbf{r})$  studied here. Third, the pseudo-elastic theory established above is only expected to hold on length scales such that  $L \gg \lambda$ . This does not necessarily hold for small piles or small silos, where the hyperbolic approach seems to give very good results [11]. It would be interesting to work out in more detail the crossover regime where  $L/\lambda$  is not large compared to one, using, for example, the formalism developed in [32]. Finally, let us note that the above theory should describe the large-scale properties of random networks of rigidly jointed struts.

We wish to thank M. Cates, E. Clément, J. Duran, G. Grest, A. Kamenev, E. Kolb, J.M. Luck, Y. Nahmias, G. Ovarlez, G. Reydellet and J. Wittmer for very useful discussions. P.C. was supported by an Aly Kaufman post-doctoral fellowship. D.L. acknowledges support from Israel Science Foundation grant 211/97 and from U.S.-Israel Binational Science Foundation grant 1999235. M.O. is supported by a DFG research fellowship.

## References

1. P.-G. de Gennes, *Physica A* **261**, 293 (1998).
2. S.B. Savage, in *Physics of Dry Granular Media*, edited by H.J. Herrmann, J.P. Hovi, S. Luding, *NATO ASI, Ser. E*, Vol. **350** (1997), p. 25.
3. J.-P. Bouchaud, P. Claudin, M.E. Cates, J.P. Wittmer, in *Physics of Dry Granular Media*, edited by H.J. Herrmann, J.P. Hovi, S. Luding, *NATO ASI, Ser. E*, Vol. **350** (1997), p. 97.
4. M.E. Cates, J.P. Wittmer, J.-P. Bouchaud, P. Claudin, *Phil. Trans. Roy. Soc. Lond. A* **356**, 2535 (1998).
5. L. Landau, E. Lifshitz, *Elasticity Theory* (Pergamon, New York, 1986).
6. G. Combe, J.-N. Roux, *Phys. Rev. Lett.* **85**, 3628 (2000).
7. J.-P. Bouchaud, M.E. Cates, P. Claudin, *J. Phys. I* **5**, 639 (1995).
8. J.P. Wittmer, P. Claudin, M.E. Cates, J.-P. Bouchaud, *Nature* **382**, 336 (1996); J.P. Wittmer, P. Claudin, M.E. Cates, *J. Phys. I* **7**, 39 (1997).
9. P. Claudin, *Ann. Phys. (Paris)*, **24**, 1 (1999).
10. R.M. Nedderman, *Statics and Kinematics of Granular Materials* (Cambridge University Press, 1992).
11. L. Vanel, P. Claudin, J.-P. Bouchaud, M.E. Cates, E. Clément, J.P. Wittmer, *Phys. Rev. Lett.* **84**, 1439 (2000).
12. M.E. Cates, J.P. Wittmer, J.-P. Bouchaud, P. Claudin, *Phys. Rev. Lett.* **81**, 1841 (1998).
13. J. Smíd, J. Novosad, *Proc. Powtech. Conference 1981*, Ind. Chem. Eng. Symp. **63**, D3V 1 (1981); R. Brockbank, J.M. Huntley, R.C. Ball, *J. Phys. II* **7**, 1521 (1997).
14. L. Vanel, D.W. Howell, D. Clark, R.P. Behringer, E. Clément, *Phys. Rev. E* **60**, R5040 (1999)
15. C.-h. Liu, S.R. Nagel, D.A. Schecter, S.N. Coppersmith, S. Majumdar, O. Narayan, T.A. Witten, *Science* **269**, 513 (1995); S.N. Coppersmith, C.-h. Liu, S. Majumdar, O. Narayan, T.A. Witten, *Phys. Rev. E* **53**, 4673 (1996). See also S. Luding, preprint.
16. J. Geng, D. Howell, E. Longhi, R.P. Behringer, G. Reydellet, L. Vanel, E. Clément, S. Luding, preprint, cond-mat/0012127.
17. S. Nagel *et al.*, in preparation.
18. V. Tkachenko, T.A. Witten, *Phys. Rev. E* **60**, 687 (1999); see also S.F. Edwards, D.V. Grinev, *Phys. Rev. Lett.* **82**, 5397 (1999).
19. G. Reydellet, E. Clément, preprint, cond-mat/0012083.
20. E. Clément, G. Reydellet, L. Vanel, D.W. Howell, J. Geng, R.P. Behringer, *XIII International Congress on Rheology, Cambridge (UK)*, Vol. **2** (British Society of Rheology, Glasgow, 2000) p. 426.
21. J.-J. Moreau, in the proceedings of the *colloque 'Physique et mécanique des matériaux granulaires'*, Champs-sur-Marne (France) (École Nationale des Ponts et Chaussées, Marne-la-Vallée, 2000) p. 199.
22. M. da Silva, J. Rajchenbach, *Nature* **406**, 70 (2000).
23. S.F. Edwards, *Physica A* **249**, 226 (1998).
24. P. Dantu, *Ann. Ponts Chaussées* **4**, 144 (1967).
25. See also the numerical simulations of F. Radjai, D.E. Wolf, M. Jean, J.J. Moreau, *Phys. Rev. Lett.* **80**, 61 (1998), and references therein.
26. V.M. Kenkre, J.E. Scott, E.A. Pease, A.J. Hurd, *Phys. Rev. E* **57**, 5841 (1998); J.E. Scott, V.M. Kenkre, A.J. Hurd, *Phys. Rev. E* **57**, 5850 (1998).
27. P. Claudin, J.-P. Bouchaud, M.E. Cates, J.P. Wittmer, *Phys. Rev. E* **57**, 4441 (1998).
28. M.C.W. van Rossum, Th.M. Nieuwenhuizen, *Rev. Mod. Phys.* **71**, 313 (1999).
29. see J. Duran, *Sables, poudres et grains* (Eyrolles Sciences, Paris, 1997); see also H.A. Makse, N. Gland, D.L. Johnson, L.M. Schwartz, *Phys. Rev. Lett.* **83**, 5070 (1999).
30. M. Otto, J. P. Bouchaud, Ph. Claudin, in preparation.
31. F. Cantelaube, J. Goddard, in *Physics of Dry Granular Media*, edited by H.J. Herrmann, J.P. Hovi, S. Luding, *NATO ASI, Ser. E*, Vol. **350** (1997) p. 123.
32. E. Amic, J.-M. Luck, Th. Nieuwenhuizen, *J. Phys. A* **29**, 4915 (1996).